

# Chain-of-Thought Reasoning Enhances In-Context Learning for LLM-Based Mobile Traffic Prediction

MohammadMahdi Ghadaksaz, Mohammad Farzanullah, *Graduate Student Member, IEEE*, Akram Bin Sediq, Ali Afana, Melike Erol-Kantarci, *Fellow, IEEE*

**Abstract**—Accurate short-term mobile traffic prediction is important for proactive resource allocation and low-latency network management in fifth generation (5G) and sixth generation (6G). While large language models (LLMs) can perform in-context learning (ICL) without task-specific retraining, naive ICL prompting may suffer from numerical instability and limited temporal reasoning when traffic dynamics fluctuate rapidly. In this paper, we propose a chain-of-thought (CoT)-enabled LLM-based mobile traffic prediction framework that operates in two phases: (i) an offline phase that constructs structured CoT demonstrations by generating *rationales* via a plan-based CoT (PCoT) pipeline (*lecture*, *plan*, and *rationale*), and (ii) an online phase that performs close to real-time prediction by retrieving the most relevant demonstrations using a similarity policy that considers both the historical throughput pattern and its short-term changes. We evaluate the proposed framework using a real-world 5G measurement dataset that includes both driving and static scenarios across diverse applications. Our numerical results reveal that the proposed 2-shot CoT-LLM can improve mean absolute error (MAE), root mean square error (RMSE) and  $R^2$ -score by up to 14.88%, 15.03%, and 22.41%, respectively, compared to the 2-shot ICL-LLM and classical baselines. Furthermore, by optimizing the number of in-context examples, we achieve additional improvements of 4.58%, 5.70%, and 4.85% in MAE, RMSE, and  $R^2$ -score, respectively.

**Index Terms**—Large language models (LLMs), chain of thought, reasoning, mobile traffic prediction, 6G.

## I. INTRODUCTION

WIRELESS mobile networks are experiencing unprecedented growth in traffic volume and variability due to the proliferation of data-intensive applications such as high-definition video streaming, cloud-based services, and interactive mobile platforms. Beyond fifth generation (5G), emerging sixth generation (6G) networks will introduce new demands from physical artificial intelligence (AI), agentic communications, extended reality, and machine-to-machine (M2M) interactions, creating more diverse and bursty traffic patterns that traditional prediction frameworks struggle to capture. Notably, AI-driven and M2M workloads are highly latency-sensitive, making accurate traffic prediction essential to proactively allocate resources and meet service-level agreements before demand surges occur [1]–[3].

Accurate traffic prediction allows network operators to transition from reactive to proactive network management. By

anticipating future traffic demands, base stations (BSs) and core network entities can perform intelligent resource allocation, congestion avoidance, and adaptive quality of service (QoS) provisioning. Moreover, predictive traffic awareness plays a central role in energy-efficient networking, mobility management, and edge intelligence, where timely decisions must be made under strict latency constraints [4], [5]. However, wireless traffic is inherently complex, as it is jointly affected by user mobility, radio channel variations, application-level behavior, and network configurations. These factors make mobile traffic prediction a challenging task, especially in realistic, large-scale deployments.

Traditional traffic prediction methods, including statistical models and classical time-series techniques, often rely on strong assumptions about stationarity and linearity, which limit their effectiveness in highly dynamic wireless environments. While machine learning (ML)-based approaches have improved prediction accuracy by capturing nonlinear dependencies, they typically require large labeled datasets, extensive offline training, and periodic retraining to remain effective when traffic characteristics shift [6]. Such requirements reduce their practicality in scenarios where traffic patterns change frequently or differ across locations and applications.

Recently, large language models (LLMs) have emerged as a flexible alternative for data-driven inference and prediction tasks beyond their original focus on natural language processing. A key advantage of LLMs is their ability to perform in-context learning (ICL), where a model can adapt to a new task by observing a small number of examples provided directly in the prompt, without updating model parameters [7]. This capability makes LLMs particularly appealing for mobile traffic prediction, as it enables rapid adaptation across diverse scenarios and reduces the need for repeated retraining. Nevertheless, naive ICL prompting may struggle with numerical stability and temporal reasoning, especially when the prediction task involves complex traffic dynamics.

In this context, reasoning has emerged as a key capability in advanced AI systems. By decomposing complex problems into intermediate logical steps, reasoning-enabled models improve generalization and interpretability. For LLMs, this capacity is tied to the quality of intermediate steps generated before the final answer. Chain-of-thought (CoT) prompting has been introduced as an effective mechanism to improve the reasoning behavior of LLMs by explicitly guiding the model through intermediate inference steps [8]. By structuring the prediction process and exposing latent reasoning paths, CoT prompting enables LLMs to better exploit historical trends and contextual signals embedded in mobile traffic data. This motivates the

MohammadMahdi Ghadaksaz, Mohammad Farzanullah, and Melike Erol-Kantarci are with the School of Electrical Engineering and Computer Science, University of Ottawa, Ottawa, ON K1N 6N5, Canada (e-mail: mghad017@uottawa.ca; mfarz086@uottawa.ca; melike.erolkantarci@uottawa.ca).

Akram Bin Sediq and Ali Afana are with Ericsson, Ottawa, K2K 2V6, Canada (e-mail: akram.bin.sediq@ericsson.com; ali.afana@ericsson.com)

exploration of CoT-enabled LLMs for wireless traffic prediction and necessitates an evaluation of their performance, robustness, and practical deployment in real-world scenarios.

### A. Related Works

1) *Mobile Traffic Prediction*: Mobile traffic prediction has been an active research topic over the past few years [9]–[13]. In particular, the authors in [9] propose a weighted moving average (WMA)-based approach for mobile traffic prediction. Similarly, [10] develops an auto regressive integrated moving average (ARIMA)-based statistical model for traffic prediction, showing that ARIMA can outperform several benchmark methods. In [11], the authors propose an long short-term memory (LSTM)-based framework to model and predict traffic patterns, where multivariate time-series prediction is performed for both one-step and longer-term predictions to evaluate how far ahead accurate predictions can be achieved. The work in [12] introduces an adaptive graph convolutional recurrent network (AGCRN) to capture fine-grained spatial and temporal correlations in traffic data, demonstrating the effectiveness of graph-based modeling. Furthermore, [13] investigates an spatiotemporal dynamic graph network (SDGNet) framework based on dynamic graph convolution (DGC) and gated linear units (GLUs) to predict traffic consumption over short-, medium-, and long-term horizons, where the results show lower prediction error compared to conventional models.

With the advancement of transformer architectures [14] and their strong ability to capture long-term dependencies, these models have also been applied to mobile traffic prediction [15]–[18]. In [15], the authors introduce a temporal fusion transformer (TFT)-based framework for wireless traffic prediction to support efficient network management and improve quality of experience (QoE). In [16], a spatial-temporal downsampling transformer neural network (STDT-Net) approach is proposed to jointly exploit temporal, local spatial, and global spatial dependencies for traffic prediction. Similarly, the studies in [17], [18] investigate spatio-temporal transformer architectures for cellular traffic prediction, further highlighting the potential of transformer-based models in this domain.

2) *LLMs in Wireless Communications*: Thanks to their strong capabilities and proven success in both academia and industry [19], LLMs have recently gained increasing attention in the wireless communications community for a wide range of prediction and detection tasks [20]–[23]. One key advantage of LLM-based approaches is that, unlike conventional transformer- or ML-based methods, they do not require task-specific retraining. While initial pre-training of LLMs depends on massive corpora available in the language domain, wireless datasets—containing signals, channel measurements, or traffic traces—remain limited in public availability and costly to collect. Consequently, parameter-free adaptation through ICL is particularly attractive for wireless tasks, where re-training on every scenario is impractical.

In [20], the authors propose an LLM-based intrusion detection framework using ICL, and their results demonstrate

acceptable detection accuracy. Similarly, the authors in [21] introduce an LLM-based mobile traffic prediction framework with a two-stage ICL example selection strategy, achieving low prediction error. In [22], a self-refined LLM is designed to iteratively correct inaccurate predictions through a three-step process, where hourly traffic is predicted using random ICL example selection. Moreover, the authors in [23] apply lightweight LLMs to intent-processing tasks, demonstrating improved network throughput and efficiency.

Several recent studies also investigate LLM fine-tuning or training from scratch for time-series prediction tasks [24], [25]. In [24], the authors employ an interpretable, prompt-tuning-based generative transformer to learn time-series representations. Furthermore, [25] proposes two fine-tuning strategies to better adapt LLMs to the characteristics of time-series data, showing that fine-tuning can outperform ICL-based methods and other prompt-engineering approaches in certain scenarios.

Although CoT prompting is still in its early stages of adoption in wireless communications, it has already been explored in several recent studies [26], [27]. In [26], the authors apply CoT to reason about the causes of performance degradation in 6G networks. Similarly, [27] investigates multiple CoT strategies, where Auto-CoT is employed for unmanned aerial vehicle (UAV) location and power allocation optimization. The results demonstrate that CoT-based methods outperform their non-CoT counterparts.

### B. Motivations & Contributions

Most existing research on wireless traffic prediction has largely overlooked the potential of LLMs. This observation is evident in several prior works [9]–[13], [15]–[18]. In particular, studies such as [9], [10] rely on simple statistical methods, which often struggle to capture complex traffic dynamics. Other works (i.e., [11]–[13], [15]–[18]) adopt data-driven approaches that depend heavily on large training datasets, which are not always available, and whose training processes can be computationally expensive and time-consuming. On the other hand, although the authors in [21], [22] have considered LLMs for traffic prediction, they have been limited to ICL, whereas the potential of CoT prompting has been unexplored. Furthermore, several studies, such as [24], [25], employ fine-tuned LLMs for time-series prediction. However, mobile traffic patterns evolve rapidly due to changes in user behavior, mobility, and application usage, which would require frequent fine-tuning and introduce additional computational overhead, complicating practical deployment in dynamic network environments. Moreover, fine-tuning still relies on the availability of task- and scenario-specific data, which may not always be readily available for all traffic conditions or deployment scenarios. In contrast, prompt-based approaches, such as ICL and CoT, do not require any model tuning, making them more flexible and easier to deploy in dynamic traffic environments. Lastly, although the works in [26], [27] employ CoT-based solutions, they do not apply this approach to mobile traffic prediction. To the best of our knowledge, this is the first time CoT-enabled LLM-based mobile traffic prediction using a structured example selection has been explored to enhance performance using a real-world 5G dataset.

The main contributions of this work can be highlighted as follows:

- 1) We propose a novel CoT-enabled LLM-based mobile traffic prediction framework that consists of an offline prompt construction phase and an online traffic prediction phase. During the offline phase, *rationales* (i.e., step-by-step guidance toward accurate traffic prediction) are generated from historical traffic data using a three-step *rationale* generation process, which serves as long-term memory to enhance prediction performance. Subsequently, during the online phase, the most similar examples are selected according to a specific selection policy, further improving the accuracy of traffic prediction.
- 2) We evaluate the impact of the number of examples on the performance of the CoT-LLM for the traffic prediction task and analyze how the example selection policy affects the results. In addition, we compare the performance of CoT with standard ICL prompting and examine the stability of both approaches under varying numbers of examples and traffic conditions.
- 3) We conduct an extensive evaluation across multiple open-weight LLMs. In particular, since many state-of-the-art LLMs are not publicly released, we show that the proposed CoT-LLM-based mobile traffic prediction framework can be implemented using open-weight models while achieving performance comparable to, or even exceeding, that of closed-weight models. By leveraging open-weight models, LLMs can be deployed locally without relying on external application programming interface (API) services, thereby significantly reducing inference latency and enabling close to real-time traffic prediction.

We demonstrate the effectiveness of the proposed solutions using a real-world 5G dataset that includes diverse practical scenarios. Our numerical results validate the effectiveness of the proposed framework. In particular, the 2-shot CoT-LLM achieves improvements of up to 14.88%, 15.03%, and 22.41% in mean absolute error (MAE), root mean square error (RMSE), and  $R^2$ -score, respectively, compared to the 2-shot ICL-LLM and classical baseline methods. Furthermore, we show that optimizing the number of in-context examples yields additional gains of 4.58%, 5.70%, and 4.85% in MAE, RMSE, and  $R^2$ -score, respectively, highlighting the importance of example selection. Finally, evaluations across multiple open-weight LLMs demonstrate that locally deployable models can achieve performance comparable to, or exceeding, closed-weight alternatives, enabling practical low-latency traffic prediction without reliance on external APIs.

### C. Organization

The remainder of this paper is organized as follows: Section II presents the discussed problem followed by the methodology in Section III. Section IV provides the numerical results and analysis, and finally Section V concludes the paper with conclusions and future works.

## II. PROBLEM DESCRIPTION

In this section, we formulate the CoT-enabled LLM-based downlink mobile traffic prediction problem for a generic traffic measurement dataset that contains downlink throughput observations along with a set of network-related contextual features.

Let us denote the downlink throughput and the  $k^{\text{th}}$  contextual feature at time step  $t$  of measurement by  $\gamma^{(t)}$  and  $c_k^{(t)}$ , respectively. A raw dataset  $\tilde{\mathcal{D}}$  with  $H$  seconds of traffic measurement is then represented as:

$$\tilde{\mathcal{D}} = \left\{ \left( \gamma^{(t)}, \mathbf{c}^{(t)} \right) \right\}_{t=1}^H, \quad (1)$$

where  $\mathbf{c}^{(t)} = [c_1^{(t)}, \dots, c_K^{(t)}] \in \mathcal{X}^K$  ( $\mathcal{X}$  denotes the mixed type data) collects the  $K$  contextual features at time step  $t$ . Due to prompt-size limitations, we use a historical window of length  $W$  seconds as the input to the prediction model. Subsequently, we define the historical throughput vector  $\mathbf{\Gamma}^{(t)}$  at time step  $t$  as:

$$\mathbf{\Gamma}^{(t)} = [\gamma^{(t)}, \gamma^{(t-1)}, \dots, \gamma^{(t-W+1)}] \in \mathbb{R}^W. \quad (2)$$

Likewise, the historical contextual information matrix  $\mathbf{C}^{(t)}$ , including  $K$  contextual features, at time step  $t$  can be written as follows:

$$\mathbf{C}^{(t)} = \begin{bmatrix} c_1^{(t)} & c_2^{(t)} & \dots & c_K^{(t)} \\ c_1^{(t-1)} & c_2^{(t-1)} & \dots & c_K^{(t-1)} \\ \vdots & \vdots & \ddots & \vdots \\ c_1^{(t-W+1)} & c_2^{(t-W+1)} & \dots & c_K^{(t-W+1)} \end{bmatrix} \in \mathcal{X}^{W \times K}. \quad (3)$$

In this case, we focus on one time step traffic prediction task, expressed as:

$$y^{(t)} = \gamma^{(t+1)}, \quad (4)$$

where using a pre-trained LLM with fixed parameters, the model is asked to output the subsequent downlink throughput and a *rationale* for its respond, formulated as:

$$\left[ \hat{y}^{(t)}, r^{(t)} \right] = f \left( \mathbf{C}^{(t)}, \mathbf{\Gamma}^{(t)} | \Theta \right), \quad (5)$$

where  $\hat{y}^{(t)}$  denotes the predicted downlink throughput,  $r^{(t)}$  is the *rationale*,  $f(\cdot)$  represents the LLM, and  $\Theta$  is the model's parameters.

Equation (5) is commonly referred to as zero-shot CoT-LLM prediction [28]. To improve the performance of zero-shot prediction, we include several known examples, each paired with a *rationale*, in the prompt. This forms an extension of zero-shot CoT, which is known as few-shot CoT [8]. The incorporation of the known examples enables the LLMs to solve new tasks without being fine-tuned or re-trained [29].

The CoT prompting differs from ICL prompting in that, in ICL, the LLM is only provided with examples, whereas in CoT approaches, the examples are accompanied by an explicit *rationale* that guides the model through the intermediate reasoning steps before producing the final prediction. Moreover, the model is explicitly instructed to *think step-by-step* before

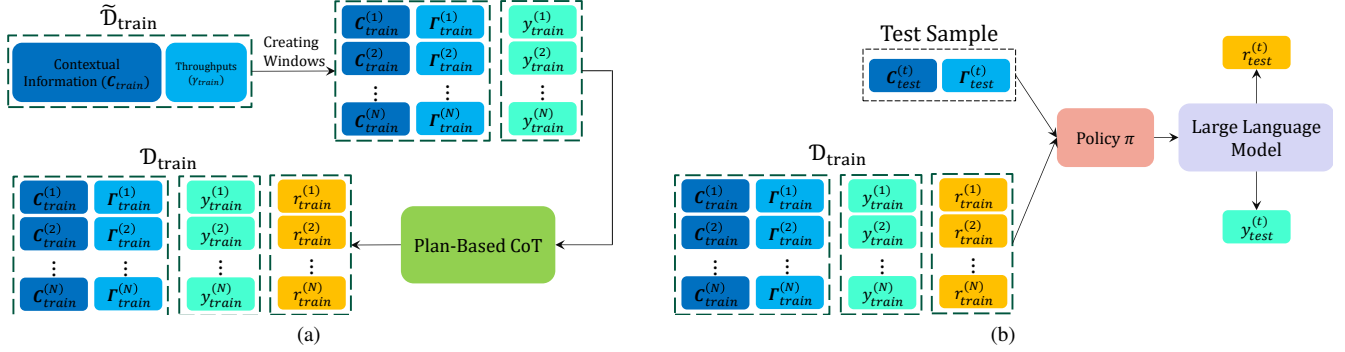


Fig. 1. Block diagram of the proposed few-shot CoT-LLM mobile traffic prediction framework. (a) offline prompt construction phase: traffic measurements are segmented into windows and fed through the PCoT pipeline to generate structured training examples with *rationales*. (b) Online traffic prediction phase: The selection policy  $\pi$  retrieves the  $M$  most relevant training examples, injects them into the LLM prompt, and produces the predicted throughput.

generating the output, which encourages the LLM to produce intermediate reasoning steps rather than jumping directly to a final answer — a technique shown to improve complex reasoning performance compared to standard ICL prompting [8], [28]. Nonetheless, in both approaches, the selection and number of examples are important and can significantly impact the overall performance.

To clearly separate the data used to construct the CoT examples from the data used for evaluation, we assume that the training examples are drawn from a processed training dataset  $\mathcal{D}_{\text{train}}$ , whereas the test samples are taken out from a separate processed test dataset  $\mathcal{D}_{\text{test}}$ , with no overlap between the two datasets. Each example in the processed training set consists of a historical downlink throughput sequence and the associated contextual information, denoted by  $\mathbf{\Gamma}_{\text{train}}^{(n)}$  and  $\mathbf{C}_{\text{train}}^{(n)}$ , respectively, along with a corresponding *rationale*  $r_{\text{train}}^{(n)}$ , and the ground-truth traffic at the next time step  $y_{\text{train}}^{(n)}$ . This training example can be written as:

$$\mathbf{E}_{\text{train}}^{(n)} = \left[ \left[ \mathbf{C}_{\text{train}}^{(n)}, \mathbf{\Gamma}_{\text{train}}^{(n)} \right], r_{\text{train}}^{(n)}, y_{\text{train}}^{(n)} \right], \quad (6)$$

where  $\mathbf{E}_{\text{train}}^{(n)}$  denotes the  $n^{\text{th}}$  example in the processed training set  $\mathcal{D}_{\text{train}} = \left\{ \mathbf{E}_{\text{train}}^{(n)} \right\}_{n=1}^N$ , where  $n \in \{1, \dots, N\}$  indexes the  $N$  training examples. The specific methodology for generating the *rationales*  $r_{\text{train}}^{(n)}$  will be discussed in Section III. Subsequently, for  $M$ -shot CoT prediction on a test sample  $\mathbf{T}_{\text{test}}^{(t)} = \left[ \mathbf{\Gamma}_{\text{test}}^{(t)}, \mathbf{C}_{\text{test}}^{(t)} \right]$  at time step  $t$ , the  $M$  examples' indices are selected using a selection policy  $\pi$  as:

$$\mathcal{I} \left( \mathbf{T}_{\text{test}}^{(t)} \right) = \pi \left( \mathbf{T}_{\text{test}}^{(t)}, \mathcal{D}_{\text{train}} \right), \quad \left| \mathcal{I} \left( \mathbf{T}_{\text{test}}^{(t)} \right) \right| = M. \quad (7)$$

Subsequently, the selected examples' set for the test sample  $\mathbf{T}_{\text{test}}^{(t)}$  can be defined as:

$$\mathcal{D}_{\text{CoT}} \left( \mathbf{T}_{\text{test}}^{(t)} \right) = \left\{ \mathbf{E}_{\text{train}}^{(m)}; m \in \mathcal{I} \left( \mathbf{T}_{\text{test}}^{(t)} \right) \right\}. \quad (8)$$

Consequently, the predicted traffic and the *rationale* using the LLM under  $M$ -shot CoT prompting can be written as:

$$\left[ \hat{y}_{\text{test}}^{(t)}, r_{\text{test}}^{(t)} \right] = f \left( \mathbf{T}_{\text{test}}^{(t)}, \mathcal{D}_{\text{CoT}} \left( \mathbf{T}_{\text{test}}^{(t)} \right) \mid \Theta \right), \quad (9)$$

where  $\hat{y}_{\text{test}}^{(t)}$  and  $r_{\text{test}}^{(t)}$  denote the predicted traffic and corresponding *rationale*.

The traffic prediction task aims to minimize the discrepancy between the predicted downlink throughput and the corresponding ground-truth throughput. For a fixed prompting configuration (policy  $\pi$  and  $M$  examples) we estimate the expected prediction error on the test set using the empirical average as:

$$\mathbb{E} \left[ \mathcal{L} \left( \hat{y}_{\text{test}}, y_{\text{test}} \right) \right] = \frac{1}{T} \sum_{t=1}^T \mathcal{L} \left( \hat{y}_{\text{test}}^{(t)}, y_{\text{test}}^{(t)} \right), \quad (10)$$

where  $T$  is the length of the test set and  $\mathcal{L}$  is the error function.

In this work, we employ CoT-enabled LLMs to optimize the loss function, aiming to accurately predict traffic at the subsequent time step. Specifically, the CoT mechanism enables the model to decompose complex temporal dependencies into intermediate reasoning steps, thereby capturing subtle variations in traffic patterns. The following section explains the proposed CoT-LLM traffic prediction algorithm.

### III. CoT-ENABLED LLM-BASED MOBILE TRAFFIC PREDICTION

In this section, we will explain the proposed CoT-LLM mobile traffic prediction algorithm. As illustrated in Fig. 1, the proposed algorithm consists of two distinct phases: (a) an offline prompt construction phase, in which a novel framework is developed to generate the *rationales* required for CoT-LLM-based traffic prediction, and (b) an online traffic prediction phase, in which the most relevant examples are selected using the policy  $\pi$  and injected into the prompt. Each of these phases will be described in detail in the following subsections.

#### A. Phase 1: Offline Prompt Construction Phase

This phase focuses on transforming the raw training dataset  $\tilde{\mathcal{D}}_{\text{train}}$  into the structured examples  $\mathbf{E}_{\text{train}}^{(n)}$ , forming the processed training dataset  $\mathcal{D}_{\text{train}}$ . As described earlier in Section II, the historical downlink throughput  $\mathbf{\Gamma}$  and associated contextual feature sequences  $\mathbf{C}$  are formed using (2) and (3), respectively. For a raw training dataset  $\tilde{\mathcal{D}}_{\text{train}}$  containing  $H$  seconds of traffic

measurements, the number of training examples  $N$  obtained with a window size  $W$  and stride  $S$  can be expressed as:

$$N = \left\lfloor \frac{H - W}{S} \right\rfloor + 1. \quad (11)$$

After forming the historical windows, we generate the *rationales* for the training data. These *rationales* can have a substantial impact on the performance of CoT-LLM mobile traffic prediction, as we will observe. In particular, rather than only providing the final answers in the examples, we include intermediate steps and the reasoning behind each response. In this way, the model can better capture the underlying patterns and decision process required for accurate prediction.

In this context, a straightforward approach for generating the *rationales* is to rely on human expertise and manually craft several reasoning steps for each example. However, this solution can become impractical due to the large size of the training data, which makes the process time-consuming. Moreover, human knowledge may be insufficient to capture all aspects of the problem, potentially resulting in low-quality *rationales*, and, consequently, performance degradation. Thus, we rely on LLMs themselves for *rationale* generation. In this case, we adopt a PCoT strategy [26], [30], whereas the examination of other strategies is left as our future work. The PCoT approach consists of three steps for *rationale* generation, shown in Fig. 2, as:

- 1) **Lecture Generation:** In this step, the model is prompted, using the *instruction*  $i_l$ , to generate a general *lecture*  $l$  based on the past traffic throughput  $\Gamma_{\text{train}}^{(n)}$ , the associated contextual information  $\mathbf{C}_{\text{train}}^{(n)}$ , and the corresponding ground-truth next-step traffic  $y_{\text{train}}^{(n)}$  for the  $n^{\text{th}}$  training example. This can be expressed as follows:

$$l = f \left( \left[ \Gamma_{\text{train}}^{(n)}, \mathbf{C}_{\text{train}}^{(n)} \right], y_{\text{train}}^{(n)}, i_l | \Theta \right). \quad (12)$$

- 2) **Plan Generation:** After acquiring the *lecture*, the model is prompted to output a general *plan*  $p$ , using the following:

$$p = f \left( l, \left[ \Gamma_{\text{train}}^{(n)}, \mathbf{C}_{\text{train}}^{(n)} \right], y_{\text{train}}^{(n)}, i_p | \Theta \right), \quad (13)$$

where  $i_p$  denotes the *instruction* for generating the *plan*.

- 3) **Rationale Generation:** Finally, using  $l$  and  $p$ , the model is prompted to generate a *rationale* as:

$$r_{\text{train}}^{(n)} = f \left( l, p, \left[ \Gamma_{\text{train}}^{(n)}, \mathbf{C}_{\text{train}}^{(n)} \right], y_{\text{train}}^{(n)}, i_r | \Theta \right). \quad (14)$$

Here,  $r_{\text{train}}^{(n)}$  represents the *rationale* associated with the  $n^{\text{th}}$  example, and  $i_r$  is the *instruction* included in the prompt to generate this *rationale*. Using  $r_{\text{train}}^{(n)}$ , we then construct the complete  $n^{\text{th}}$  training example  $\mathbf{E}_{\text{train}}^{(n)}$  according to (6).

Notably, the *instructions*  $i_l$ ,  $i_p$ , and  $i_r$  are provided in Fig. 2. By repeating this process for all samples, we construct the processed training dataset  $\mathcal{D}_{\text{train}}$  as:

$$\mathcal{D}_{\text{train}} = \{ \mathbf{E}_{\text{train}}^{(n)} \}_{n=1}^N. \quad (15)$$

The summary of the offline prompt construction phase can be found in Algorithm 1.

---

**Algorithm 1: Offline Prompt Construction Phase**


---

**Input:**  $\hat{\mathcal{D}}_{\text{train}}, H, W, S, f(\cdot | \Theta), i_l, i_p,$  and  $i_r$ .  
**Output:**  $\mathcal{D}_{\text{train}}$ .

```

1 Initialize  $\mathcal{D}_{\text{temp}} \leftarrow \emptyset$ ;
2  $n \leftarrow 0$ ;
3 for  $t = W; t \leq H - 1; t \leftarrow t + S$  do
4    $n \leftarrow n + 1$ ;
5   Construct  $\Gamma^{(t)}$  and  $\mathbf{C}^{(t)}$  using (2) and (3);
6    $\Gamma_{\text{train}}^n \leftarrow \Gamma^{(t)}$ ;
7    $\mathbf{C}_{\text{train}}^n \leftarrow \mathbf{C}^{(t)}$ ;
8    $y_{\text{train}}^n \leftarrow \gamma^{(t+1)}$ ;
9    $\mathcal{D}_{\text{temp}} \leftarrow \mathcal{D}_{\text{temp}} \cup \{ (\mathbf{C}_{\text{train}}^n, \Gamma_{\text{train}}^n, y_{\text{train}}^n) \}$ ;
10 end
11  $N \leftarrow n$ ;
12 Initialize  $\mathcal{D}_{\text{train}} \leftarrow \emptyset$ ;
13 for  $n = 1; n \leq N; n \leftarrow n + 1$  do
14   Retrieve  $(\mathbf{C}_{\text{train}}^n, \Gamma_{\text{train}}^n, y_{\text{train}}^n)$  from  $\mathcal{D}_{\text{temp}}$ ;
15   Generate  $l$  using (12);
16   Generate  $p$  using (13);
17   Generate  $r_{\text{train}}^n$  using (14);
18   Construct  $\mathbf{E}_{\text{train}}^n$  using (6);
19    $\mathcal{D}_{\text{train}} \leftarrow \mathcal{D}_{\text{train}} \cup \{ \mathbf{E}_{\text{train}}^n \}$ ;
20 end
21 return  $\mathcal{D}_{\text{train}}$ ;

```

---

### B. Phase 2: Online Traffic Prediction

This phase involves online traffic prediction, where using the policy  $\pi$ , we select the best- $M$  examples for  $M$ -shot CoT-LLM prediction.

In the first step, we explain the policy  $\pi$ , which follows a rule to retrieve examples that are most *relevant* to the current test window. In particular, given the test input pair  $\mathbf{T}_{\text{test}}^{(t)} = [\Gamma_{\text{test}}^{(t)}, \mathbf{C}_{\text{test}}^{(t)}]$  at time step  $t$ , we score each candidate training example  $[\Gamma_{\text{train}}^{(n)}, \mathbf{C}_{\text{train}}^{(n)}]$ ,  $n \in \{1, \dots, N\}$ , using a two-part distance that jointly captures the similarity of (i) the raw historical downlink throughput shape and (ii) its short-term dynamics (first-order increments). This design is motivated by the observation that, under an ICL-as-kernel-regression view, demonstrations that are *more similar* to the test input tend to yield smaller prediction errors.

We first define the incremental (first-difference) throughput vector associated with a  $W$ -second historical window as:

$$\Delta \Gamma^{(t)} = \left[ \gamma^{(t)} - \gamma^{(t-1)}, \gamma^{(t-1)} - \gamma^{(t-2)}, \dots, \gamma^{(t-W+2)} - \gamma^{(t-W+1)} \right] \in \mathbb{R}^{W-1}. \quad (16)$$

Then, for each training candidate  $n$ , we compute two Euclidean distances as follows:

$$e_1(t, n) = \left\| \Gamma_{\text{test}}^{(t)} - \Gamma_{\text{train}}^{(n)} \right\|_2, \quad (17)$$

$$e_2(t, n) = \left\| \Delta \Gamma_{\text{test}}^{(t)} - \Delta \Gamma_{\text{train}}^{(n)} \right\|_2, \quad (18)$$

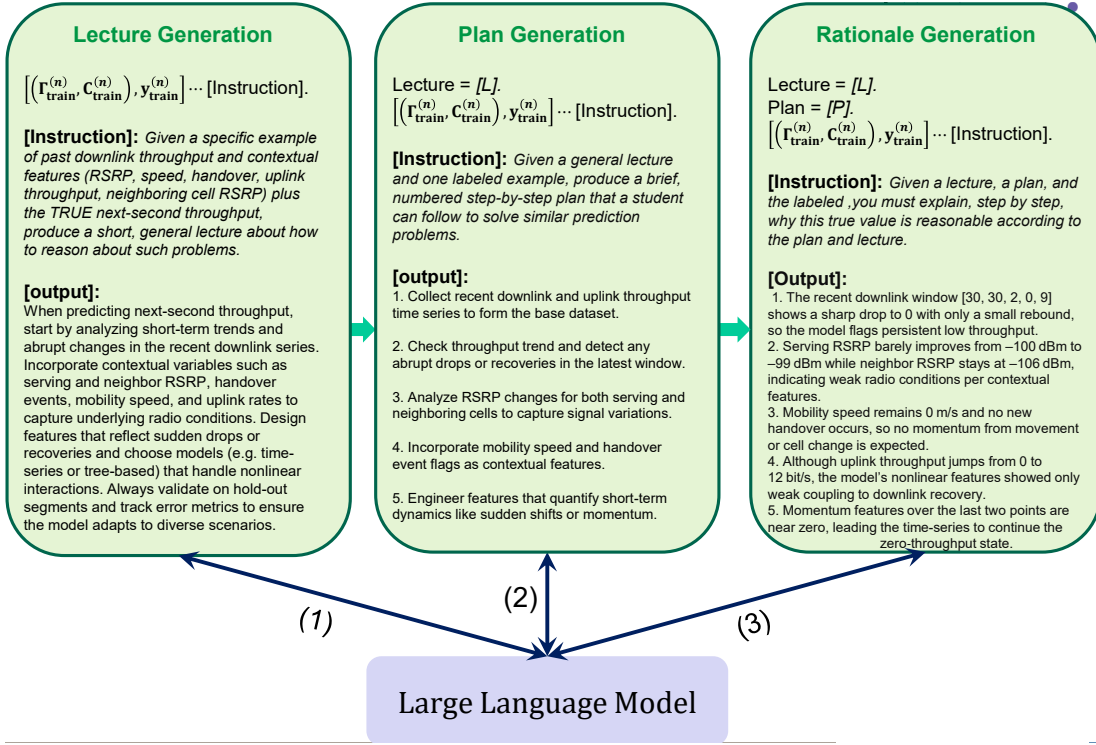


Fig. 2. The block diagram of PCoT for *rationale* generation.

and combine them into a single score [21]:

$$\mathcal{E}(t, n) = e_1(t, n) + e_2(t, n). \quad (19)$$

Finally, the policy  $\pi$  selects the indices of the  $M$  most effective examples (smallest  $\mathcal{E}(t, n)$ ):

$$\mathcal{I}(\mathbf{T}_{\text{test}}^{(t)}) = \pi(\mathbf{T}_{\text{test}}^{(t)}, \mathcal{D}_{\text{train}}) = \arg \min_{\substack{\mathcal{I} \subseteq \{1, \dots, N\} \\ |\mathcal{I}| = M}} \sum_{n \in \mathcal{I}} \mathcal{E}(t, n). \quad (20)$$

The resulting  $M$  examples are then assembled (together with their labels/rationales produced in Phase 1) to form  $\mathcal{D}_{\text{CoT}}(\mathbf{T}_{\text{test}}^{(t)})$  using (8). Consequently, these components are injected into the prompt using (9) for the CoT-LLM inference. The summary of the online phase is provided in Algorithm 2.

#### IV. NUMERICAL RESULTS

In this section, we present the numerical results obtained from our simulations. We investigate downlink mobile traffic prediction for real-world 5G user services using the measurement dataset in [31], which includes both static and driving scenarios across diverse applications, such as file downloading and video streaming (e.g., Amazon Prime), captured from operational networks. The dataset is publicly available and provides downlink throughput measurements together with various network-related contextual features, including channel metrics and neighboring-cell metrics. Specifically, it contains four categories of contextual information—throughput measurements, channel-related metrics, neighboring-cell metrics, and additional context indicators—resulting in a total of 25 contextual features. For the downlink traffic prediction

---

#### Algorithm 2: Online Prediction Phase

---

**Input:**  $\mathcal{D}_{\text{train}}, \mathbf{T}_{\text{test}}^{(t)}, M, \pi$ , and  $f(\cdot | \Theta)$ .  
**Output:**  $[\hat{y}_{\text{test}}^{(t)}, r_{\text{test}}^{(t)}]$ .

- 1 Construct  $\Delta \Gamma_{\text{test}}^{(t)}$  using (16);
  - 2 **for**  $n = 1; n \leq N; n \leftarrow n + 1$  **do**
  - 3     Retrieve  $\mathbf{I}_{\text{train}}^{(n)}$  from  $\mathcal{D}_{\text{temp}}$ ;
  - 4     Construct  $\Delta \Gamma_{\text{train}}^{(n)}$  using (16);
  - 5     set  $e_1(t, n)$  using (17);
  - 6     set  $e_2(t, n)$  using (18);
  - 7     Form  $\mathcal{E}(t, n)$  using (19);
  - 8 **end**
  - 9 Select indices  $\mathcal{I}(\mathbf{T}_{\text{test}}^{(t)})$  using (20);
  - 10 Form  $\mathcal{D}_{\text{CoT}}(\mathbf{T}_{\text{test}}^{(t)})$  using (8);
  - 11 Generate  $[\hat{y}_{\text{test}}^{(t)}, r_{\text{test}}^{(t)}]$  using (9);
  - 12 **return**  $[\hat{y}_{\text{test}}^{(t)}, r_{\text{test}}^{(t)}]$ ;
- 

task, in addition to the historical downlink throughput, we focus on  $K = 5$  contextual features: uplink throughput, the reference signal received power (RSRP) of the serving cell, the RSRP of a neighboring cell, the network mode, and handover occurrence. This feature selection follows the feature-ranking analysis reported in [32], where importance scores were computed using the same dataset, and the five most impactful features were identified.

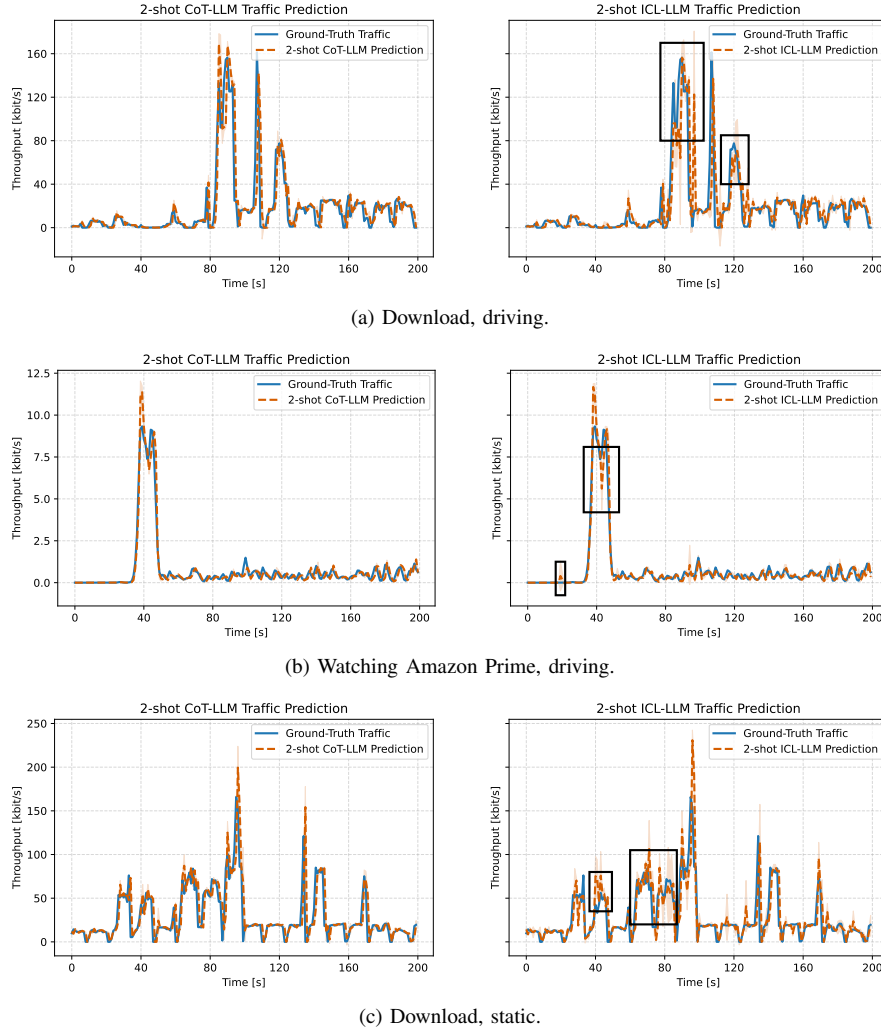


Fig. 3. Predicted traffic versus ground-truth traffic for 2-shot CoT-LLM and 2-shot ICL-LLM.

For these experiments, we use the o4-mini model [33] as the main LLM and the same model is employed in both the offline and online phases. To improve the reliability of the results, all simulations are conducted over 5 independent runs, and the reported performance metrics are averaged across these runs. We split the raw dataset equally into training and testing subsets with no overlap between them, where the first  $T = 200$  seconds of each test trace are used for testing, and the remaining samples are reserved for training. The evaluation is conducted across multiple traffic scenarios, including downloading while driving, watching Amazon Prime while driving, and downloading in a static setting. Under this setup, the training data consist of  $H = 664$  seconds for the downloading-while-driving scenario,  $H = 1569$  seconds for the downloading-in-static scenario, and  $H = 588$  seconds for the Amazon Prime-while-driving scenario. Moreover, for data processing, we use a window size of  $W = 5$  and a stride of  $S = 1$  for all results reported in this section.

#### A. Evaluation Metrics

To evaluate the performance of various traffic prediction algorithms, we consider three main metrics as:

- **MAE:** This metric quantifies the average absolute deviation between the predicted and ground-truth values. It is computed as:

$$\text{MAE} = \frac{1}{T} \sum_{t=1}^T \left| \hat{y}^{(t)} - y^{(t)} \right|, \quad (21)$$

where higher MAE indicates lower prediction precision.

- **RMSE:** This metric calculates the standard deviation of the predicted value, where similar to MAE, higher values show weaker predictions. This metric can be expressed as:

$$\text{RMSE} = \sqrt{\frac{1}{T} \sum_{t=1}^T (\hat{y}^{(t)} - y^{(t)})^2}. \quad (22)$$

- **R<sup>2</sup>-score:** This metric measures the proportion of the variance in the ground-truth values that is explained by the predictions, indicating how well the model fits the

TABLE I  
SUMMARY OF PERFORMANCE ON TEST DATA ACROSS SCENARIOS (MEAN  $\pm$  STD OVER 5 RUNS).

Method	Download (Driving)			Amazon Prime (Driving)			Download (Static)		
	MAE $\downarrow$	RMSE $\downarrow$	$R^2$ $\uparrow$	MAE $\downarrow$	RMSE $\downarrow$	$R^2$ $\uparrow$	MAE $\downarrow$	RMSE $\downarrow$	$R^2$ $\uparrow$
2-shot CoT-LLM (ours)	<b>8.039 <math>\pm</math> 0.257</b>	<b>18.552 <math>\pm</math> 0.377</b>	<b>0.639 <math>\pm</math> 0.015</b>	0.230 $\pm$ 0.008	<b>0.447 <math>\pm</math> 0.025</b>	<b>0.936 <math>\pm</math> 0.007</b>	<b>9.799 <math>\pm</math> 0.303</b>	<b>21.237 <math>\pm</math> 0.898</b>	<b>0.458 <math>\pm</math> 0.046</b>
2-shot ICL-LLM [21]	9.235 $\pm$ 0.216	21.341 $\pm$ 0.17	0.522 $\pm$ 0.053	<b>0.222 <math>\pm</math> 0.014</b>	0.489 $\pm$ 0.029	0.924 $\pm$ 0.009	11.171 $\pm$ 0.334	22.324 $\pm$ 1.458	0.399 $\pm$ 0.078
Zero-shot CoT-LLM	8.891 $\pm$ 0.380	22.058 $\pm$ 2.940	0.483 $\pm$ 0.140	0.254 $\pm$ 0.014	0.481 $\pm$ 0.038	0.926 $\pm$ 0.012	12.770 $\pm$ 0.454	23.760 $\pm$ 1.194	0.321 $\pm$ 0.067
Zero-shot ICL-LLM [21]	9.424 $\pm$ 0.533	23.214 $\pm$ 4.193	0.421 $\pm$ 0.220	0.269 $\pm$ 0.022	0.528 $\pm$ 0.064	0.910 $\pm$ 0.021	13.779 $\pm$ 0.543	25.275 $\pm$ 1.303	0.232 $\pm$ 0.077
simple moving average (SMA)	12.385 $\pm$ 0.000	24.745 $\pm$ 0.000	0.359 $\pm$ 0.000	0.419 $\pm$ 0.000	1.098 $\pm$ 0.000	0.615 $\pm$ 0.000	16.412 $\pm$ 0.000	25.168 $\pm$ 0.000	0.240 $\pm$ 0.000
WMA [9]	10.584 $\pm$ 0.000	22.041 $\pm$ 0.000	0.491 $\pm$ 0.000	0.365 $\pm$ 0.000	0.915 $\pm$ 0.000	0.732 $\pm$ 0.000	14.051 $\pm$ 0.000	22.927 $\pm$ 0.000	0.369 $\pm$ 0.000
ARIMA [10]	10.757 $\pm$ 0.000	22.385 $\pm$ 0.580	0.466 $\pm$ 0.000	0.288 $\pm$ 0.000	0.665 $\pm$ 0.000	0.859 $\pm$ 0.000	14.854 $\pm$ 0.000	25.034 $\pm$ 0.000	0.248 $\pm$ 0.000
Kalman Filter	10.400 $\pm$ 0.000	21.488 $\pm$ 0.000	0.516 $\pm$ 0.000	0.355 $\pm$ 0.000	0.896 $\pm$ 0.000	0.744 $\pm$ 0.000	13.775 $\pm$ 0.000	22.259 $\pm$ 0.000	0.405 $\pm$ 0.000

data. It can be calculated as:

$$R^2\text{-score} = 1 - \frac{\sum_{t=1}^T (y^{(t)} - \hat{y}^{(t)})^2}{\sum_{t=1}^T (y^{(t)} - \bar{y})^2}, \quad \bar{y} = \frac{1}{T} \sum_{t=1}^T y^{(t)}. \quad (23)$$

The  $R^2$ -score ranges between  $-\infty$  to 1, where higher values are an indication of a better prediction. Notably, an  $R^2$ -score of 0 indicates that the model performs no better than simply predicting the mean of the ground-truth values.

### B. CoT-LLM Mobile Traffic Prediction

In the first step, we evaluate the performance of the proposed CoT-LLM mobile traffic prediction approach against existing benchmarks across multiple scenarios. Fig. 3 illustrates the predicted traffic alongside the ground-truth traffic for three cases—namely, downloading while driving, watching Amazon Prime while driving, and downloading in a static setting—where a 2-shot CoT-LLM is compared with the 2-shot ICL-LLM baseline in [21], where the authors consider plain ICL using a similar example selection policy for traffic prediction. At this stage, we consider a 2-shot setup (two in-prompt examples) since it achieved an acceptable performance in [21]. We discuss the impact of number of examples  $M$  in the later subsections. It can be seen that the proposed 2-shot CoT-LLM achieve a better prediction compared to the 2-shot ICL-LLM, where the higher error parts are highlighted for ICL-LLM in Fig. 3.

To further assess performance, we report the MAE, RMSE, and  $R^2$ -score of the 2-shot CoT-LLM and 2-shot ICL-LLM [21] in Table I. Furthermore, in this table, we consider more benchmarks:

- 1) **zero-shot CoT-LLM:** The CoT prompting without injecting examples, where the model is explicitly asked to *think step-by-step* before outputting the traffic.
- 2) **zero-shot ICL-LLM:** The plain ICL without the in-context examples discussed in [21].
- 3) **SMA:** The average of  $W = 5$  seconds of previous traffic throughput.
- 4) **WMA [9]:** The weighted average with incremental weights of the  $W = 5$  seconds of past traffic.

- 5) **ARIMA:** The auto regressive-based traffic prediction approach discussed in [10].
- 6) **Kalman Filter:** The Kalman filter using a local level model with recursive state updates.

Overall, the proposed 2-shot CoT-LLM achieves the best performance across considered scenarios. For instance, over downloading while driving setting, the proposed 2-shot CoT-LLM algorithm attains an average MAE of 8.039, RMSE of 18.552, and  $R^2$ -score of 0.639, whereas the next-best algorithm, 2-shot ICL-LLM, achieves an average 9.235 MAE, 21.341 RMSE, and 0.522  $R^2$ -score. This means that using CoT-LLM can boost the MAE, RMSE, and  $R^2$ -score by 14.88%, 15.03%, and 22.41%, respectively. While a similar trend can be observed in the other settings, it is worth noting that only in watching Amazon Prime while driving the 2-shot ICL-LLM [21] achieves a slightly lower MAE (by 3.60%); however, the proposed 2-shot CoT-LLM still improves the RMSE and  $R^2$ -score by 9.4% and 1.3%, respectively. This can be attributed to the fact that this scenario, illustrated in Fig. 3b, is easier to predict; consequently, the performance of ICL-LLM and CoT-LLM is closer to each other.

This table also also highlights the benefit of few-shot learning compared to zero-shot learning. Particularly, for instance in downloading while driving scenario, the 2-shot CoT-LLM improves upon the zero-shot CoT-LLM by 10.60%, 18.90%, and 32.30% in terms of MAE, RMSE, and  $R^2$ -score, respectively. A similar improvement trend is also observed when comparing 2-shot ICL-LLM and zero-shot ICL-LLM.

Compared to classical benchmarks, the performance gap becomes even more evident. For example, in downloading while static setup, the 2-shot CoT-LLM improves the MAE, RMSE, and  $R^2$ -score by 38.26%, 5.82%, and 17.89%, respectively, compared to WMA [9]. Similarly, for the same setup, the 2-shot CoT-LLM enhances the Kalman filter performance by 35.34%, 15.58%, and 7.41% on MAE, RMSE, and  $R^2$ -score, respectively.

It is important to note that the achieved ranges of MAE, RMSE, and  $R^2$ -score vary across different scenarios. This is mainly due to differences in the downlink throughput range and the level of traffic fluctuation in each setting, which directly affect the difficulty of the prediction task. For instance, in the Amazon Prime while driving scenario, all benchmarks attain relatively high  $R^2$ -scores and low RMSE and MAE,

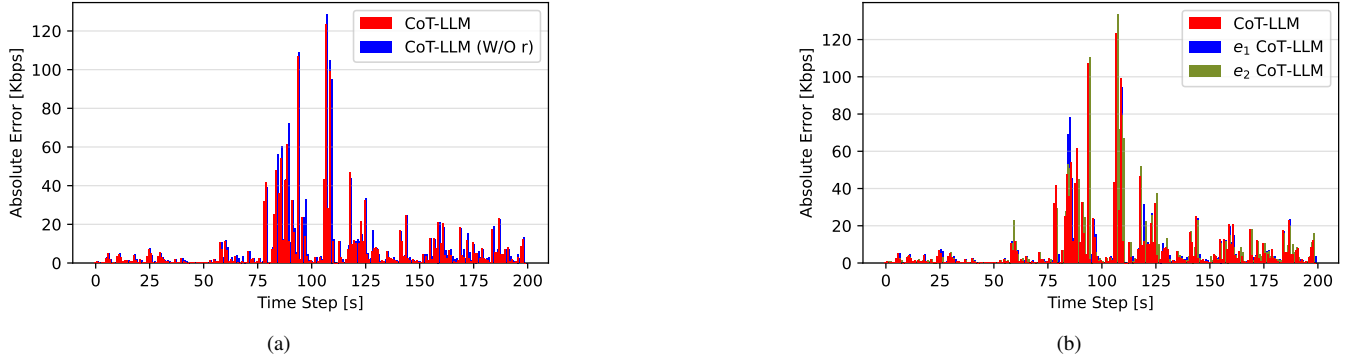


Fig. 4. The absolute error for (a) 2-shot CoT-LLM without *rationales* and (b) various selection policies.

indicating a more predictable traffic pattern. In contrast, for downloading in a static scenario, the  $R^2$ -score drops to nearly half for all methods, which suggests a highly fluctuating traffic trend and a more challenging prediction environment.

### C. Ablation Study

In this subsection, we conduct an ablation study to systematically evaluate the contribution of each component in the proposed 2-shot CoT-LLM framework for mobile traffic prediction. Without loss of generality, the downloading-while-driving scenario is used as a representative example, as similar performance trends are observed across other scenarios. Specifically, we examine the impact of the following elements within the selection policy  $\pi$  and the use of *rationales*:

- 1) The selection criterion  $e_1$  in (17).
- 2) The selection criterion  $e_2$  in (18).
- 3) The inclusion of *rationales* in the prompt.

Figure 4 illustrates the absolute prediction error for all considered variants. In particular, Fig. 4a compares the proposed 2-shot CoT-LLM against a baseline in which the *rationales* are omitted from the prompt, i.e.,

$$\left[ \hat{y}_{\text{test}}^{(t)}, r_{\text{test}}^{(t)} \right] = f \left( \mathbf{T}_{\text{test}}^{(t)}, [\mathbf{F}, \mathbf{C}, y] \mid \Theta \right). \quad (24)$$

Similarly, Fig. 4b reports the absolute error when *rationales* are retained, but either  $e_1$  or  $e_2$  is removed from the selection policy  $\pi$ . To quantitatively assess the contribution of each component, the corresponding MAE, RMSE, and  $R^2$ -score for all ablation variants are summarized in Table II.

The results indicate that all components positively contribute to the overall prediction performance. For example, excluding the *rationales* from the prompt leads to performance degradations of  $-7.04\%$ ,  $-17.34\%$ , and  $-29.09\%$  in terms of MAE, RMSE, and  $R^2$ -score, respectively, compared to the full 2-shot CoT-LLM configuration. Likewise, removing criterion  $e_1$  from the selection policy  $\pi$  results in performance drops of  $-0.30\%$  in MAE,  $-3.35\%$  in RMSE, and  $-3.09\%$  in  $R^2$ -score.

Notably, the inclusion of *rationales* yields the most significant performance gains. While modifications to the selection policy  $\pi$  introduce measurable degradation, their impact is substantially smaller than that caused by removing the *rationales*.

TABLE II

AN ABLATION STUDY ON THE IMPACT OF EACH COMPONENT COMPARED TO THE PROPOSED 2-SHOT CoT-LLM.

Method	Obtained			Average Change		
	MAE ↓	RMSE ↓	$R^2$ ↑	MAE	RMSE	$R^2$
CoT-LLM	$8.039 \pm 0.257$	$18.552 \pm 0.377$	$0.639 \pm 0.015$	—	—	—
CoT-LLM (W/O $r$ )	$8.605 \pm 0.605$	$21.769 \pm 3.220$	$0.495 \pm 0.149$	$-7.04\%$	$-17.34\%$	$-29.09\%$
$e_1$ CoT-LLM	$8.063 \pm 0.189$	$19.174 \pm 0.245$	$0.615 \pm 0.010$	$-0.30\%$	$-3.35\%$	$-3.09\%$
$e_2$ CoT-LLM	$8.327 \pm 0.202$	$19.865 \pm 0.340$	$0.601 \pm 0.017$	$-3.58\%$	$-7.08\%$	$-6.32\%$

This observation underscores the critical role of structured reasoning information in enhancing the effectiveness of CoT-LLM based prompting for mobile traffic prediction.

### D. Number of Examples

This subsection investigates the impact of the number of in-context examples on the performance of CoT-LLM and ICL-LLM-based traffic prediction. The corresponding simulation results are presented in Fig. 5 and Table III. The results demonstrate that increasing the number of examples does not necessarily lead to consistent performance improvements for either approach. In fact, an excessive number of examples can degrade prediction accuracy.

For the downloading-while-driving scenario, performance improves as the number of examples increases up to  $M = 5$ , beyond which further increases lead to noticeable degradation. By optimally selecting the number of examples, the prediction performance reaches MAE = 7.687, RMSE = 17.755, and an  $R^2$ -score of 0.670. This corresponds to improvements of 4.58%, 5.70%, and 4.85% in MAE, RMSE, and  $R^2$ -score, respectively, compared to the 2-shot CoT-LLM baseline. In contrast, for the watching Amazon Prime while driving scenario, reducing the number of examples to  $M = 1$  yields superior overall performance. While this reduction leads to a 3.47% degradation in MAE, it improves the RMSE and  $R^2$ -score by 2.05% and 0.20%, respectively, as compared to 2-shot CoT-LLM.

When compared to the ICL-LLM baseline, the proposed 5-shot CoT-LLM achieves a substantial performance gain in the downloading-while-driving scenario, outperforming ICL-LLM by 20.27% in terms of the  $R^2$ -score. However, after optimizing the number of examples for both approaches, ICL-

TABLE III  
SUMMARY OF PERFORMANCE ON TEST DATA WITH DIFFERENT NUMBER OF EXAMPLES (MEAN  $\pm$  STD OVER 5 RUNS).

Download (Driving)									
Method	Metric	$M = 0$	$M = 1$	$M = 2$	$M = 3$	$M = 4$	$M = 5$	$M = 6$	$M = 7$
$M$ -shot CoT-LLM	MAE $\downarrow$	8.891 $\pm$ 0.380	8.310 $\pm$ 0.161	8.039 $\pm$ 0.257	7.786 $\pm$ 0.089	7.853 $\pm$ 0.315	<b>7.687 <math>\pm</math> 0.136</b>	7.816 $\pm$ 0.274	7.748 $\pm$ 0.092
	RMSE $\downarrow$	22.058 $\pm$ 2.940	19.697 $\pm$ 0.728	18.551 $\pm$ 0.377	18.027 $\pm$ 0.324	17.957 $\pm$ 0.578	<b>17.755 <math>\pm</math> 0.579</b>	18.392 $\pm$ 0.633	18.465 $\pm$ 0.437
	R <sup>2</sup> $\uparrow$	0.483 $\pm$ 0.140	0.593 $\pm$ 0.030	0.639 $\pm$ 0.015	0.660 $\pm$ 0.012	0.662 $\pm$ 0.022	<b>0.670 <math>\pm</math> 0.022</b>	0.645 $\pm$ 0.024	0.643 $\pm$ 0.017
$M$ -shot ICL-LLM [21]	MAE $\downarrow$	9.424 $\pm$ 0.533	9.326 $\pm$ 0.707	9.235 $\pm$ 0.216	9.243 $\pm$ 0.251	9.168 $\pm$ 0.477	9.156 $\pm$ 0.818	9.228 $\pm$ 0.575	9.049 $\pm$ 0.848
	RMSE $\downarrow$	23.214 $\pm$ 4.193	21.782 $\pm$ 2.854	21.341 $\pm$ 1.169	21.027 $\pm$ 0.638	20.750 $\pm$ 1.614	20.461 $\pm$ 2.214	20.819 $\pm$ 2.133	21.232 $\pm$ 2.879
	R <sup>2</sup> $\uparrow$	0.421 $\pm$ 0.220	0.496 $\pm$ 0.129	0.522 $\pm$ 0.053	0.537 $\pm$ 0.028	0.547 $\pm$ 0.070	0.557 $\pm$ 0.098	0.542 $\pm$ 0.088	0.521 $\pm$ 0.128

Amazon Prime (Driving)									
Method	Metric	$M = 0$	$M = 1$	$M = 2$	$M = 3$	$M = 4$	$M = 5$	$M = 6$	$M = 7$
$M$ -shot CoT-LLM	MAE $\downarrow$	0.254 $\pm$ 0.014	0.238 $\pm$ 0.010	0.230 $\pm$ 0.008	0.230 $\pm$ 0.007	0.240 $\pm$ 0.013	0.250 $\pm$ 0.014	0.246 $\pm$ 0.009	0.255 $\pm$ 0.004
	RMSE $\downarrow$	0.481 $\pm$ 0.038	0.438 $\pm$ 0.033	0.447 $\pm$ 0.025	0.444 $\pm$ 0.016	0.469 $\pm$ 0.039	0.517 $\pm$ 0.042	0.501 $\pm$ 0.018	0.528 $\pm$ 0.033
	R <sup>2</sup> $\uparrow$	0.926 $\pm$ 0.012	0.938 $\pm$ 0.009	0.936 $\pm$ 0.007	0.937 $\pm$ 0.004	0.929 $\pm$ 0.012	0.914 $\pm$ 0.014	0.920 $\pm$ 0.006	0.911 $\pm$ 0.011
$M$ -shot ICL-LLM [21]	MAE $\downarrow$	0.269 $\pm$ 0.022	<b>0.198 <math>\pm</math> 0.013</b>	0.222 $\pm$ 0.006	0.207 $\pm$ 0.014	0.226 $\pm$ 0.016	0.242 $\pm$ 0.009	0.252 $\pm$ 0.036	0.235 $\pm$ 0.012
	RMSE $\downarrow$	0.527 $\pm$ 0.063	<b>0.390 <math>\pm</math> 0.043</b>	0.489 $\pm$ 0.029	0.437 $\pm$ 0.060	0.462 $\pm$ 0.038	0.550 $\pm$ 0.045	0.599 $\pm$ 0.181	0.524 $\pm$ 0.054
	R <sup>2</sup> $\uparrow$	0.910 $\pm$ 0.021	<b>0.951 <math>\pm</math> 0.010</b>	0.923 $\pm$ 0.009	0.938 $\pm$ 0.016	0.931 $\pm$ 0.011	0.903 $\pm$ 0.016	0.877 $\pm$ 0.078	0.912 $\pm$ 0.019

LLM exhibits a marginal 1.39% improvement over CoT-LLM in watching Amazon Prime and driving setting. In particular, when comparing the permutation entropy (PE) (which measures the irregularity of a time series) [34] of these two settings, we observe that the downloading while driving traffic exhibits a higher normalized PE than the watching Amazon Prime while driving traffic, with  $H_{PE}^{norm} = 0.780$  and  $H_{PE}^{norm} = 0.701$ , respectively<sup>1</sup>. This indicates a larger diversity of local ordinal patterns and, consequently, higher short-term irregularity in the downloading while driving setting. Such increased temporal complexity suggests that this scenario is intrinsically more challenging to predict, which is consistent with the larger performance gain achieved by the proposed CoT-LLM in this case. Conversely, the lower PE of watching Amazon Prime while driving implies a relatively more regular structure, for which standard ICL-LLM prompting remains competitive and can yield a slight advantage after per-scenario tuning. Notably, the overall performance of the two methods becomes very close for the later setting, with differences remaining within the confidence intervals of both algorithms.

Finally, an important advantage of the CoT-LLM approach is its significantly improved prediction stability. In particular, the variance of the  $R^2$ -score is reduced by 65.36% and 58.33% for the downloading-while-driving and watching-Amazon-Prime-while-driving scenarios, respectively. This substantial reduction in variance highlights the robustness and reliability of the proposed CoT-LLM framework for mobile traffic prediction.

### E. Model Comparisons

In this section, we present the performance of the proposed CoT-LLM mobile traffic prediction framework across additional LLMs. In particular, while the o4-mini model achieves

<sup>1</sup>The normalized PE value lies in  $[0, 1]$ , where larger values indicate a higher diversity of local ordinal patterns and, therefore, a less locally predictable (more irregular) time series.

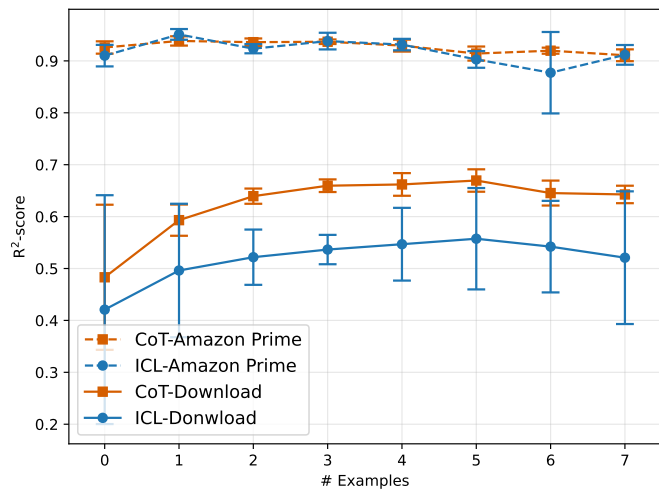


Fig. 5.  $R^2$ -score versus number of examples  $M$ .

acceptable performance, its weights are not publicly accessible, which limits its deployment to the OpenAI API. This reliance can be both costly and time-consuming, since real-time traffic prediction may be affected by the communication and processing delays between the BS/network provider and the OpenAI service. Thus, we evaluate the proposed approach using several open-weight models that can be deployed directly at the network provider. In particular, we consider the following models:

- 1) Ministral 3 3B [35].
- 2) Qwen 3 8B [36].
- 3) Phi 4 reasoning 14B [37].

These models are selected to reflect different model sizes and providers, which facilitates a more structured comparison across both dimensions. In particular, establishing performance baselines for one provider helps benchmark and interpret results when comparing models of varying sizes across different

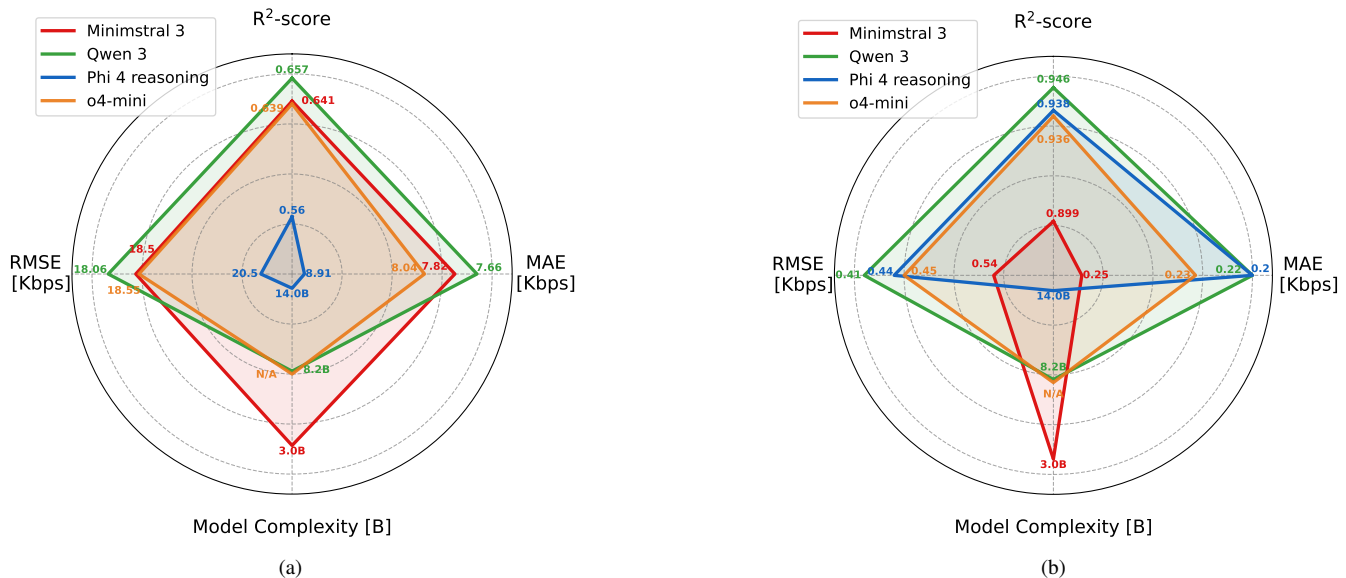


Fig. 6. Performance analysis of various LLMs for 2-shot CoT-LLM in (a) downloading while driving and (b) watching Amazon Prime while driving.

providers<sup>2</sup>.

In this paper, we use  $M = 2$  examples for all models to ensure a fair comparison, while the model-specific optimization of example selection is left for future work. Moreover, since the o4-mini LLM is not open-weight, its exact number of parameters is not publicly disclosed; therefore, to avoid inaccurate approximations, we leave the *Model Complexity* entry for o4-mini blank. Finally, each model relies on its own generated *rationales*, i.e., the offline phase is performed separately for each model.

For ease of comparison, all four axes in Fig. 6 are plotted so that a larger enclosed area corresponds to better overall performance. Specifically,  $R^2$ -score is plotted directly, where outward direction indicates higher values and better performance. On the other hand, MAE, RMSE, and *Model Complexity* are inverted on their respective axes, where outward direction indicates lower error or fewer parameters, representing better performance. Overall, for each parameter, the axes are set up such that values closer to the outer circle represent better performance. For each metric, the figure highlights the average value over five independent runs. It can be observed that Qwen 3 8B achieves the best overall performance across the considered settings, outperforming the o4-mini model. For instance, the Qwen 3 8B attains MAE of 7.66, RMSE of 18.05, and  $R^2$ -score of 0.657, whereas o4-mini model achieves an MAE of 8.04, RMSE of 18.55, and  $R^2$ -score of 0.639.

Notably, the smallest model, Minimstral 3 3B, achieves performance close to Qwen 3 8B, reaching 97.95%, 97.62%, and 97.56%, of Qwen 3 8B in terms of MAE, RMSE, and  $R^2$ -score, respectively, while using only 36.59% of the parameters. This indicates that strong performance can be obtained even with compact models.

However, these results also show that increasing model size does not necessarily improve performance and may even lead

to degradation. In the same setting, the Phi 4 reasoning with 14B parameters achieves only 85.97%, 88.05%, and 85.23% of Qwen 3 8B in terms of MAE, RMSE, and  $R^2$ -score, respectively. Overall, the results suggest that medium-sized models can offer the best trade-off between accuracy and complexity, while smaller models can be deployed with only minor performance loss for a more cost-efficient approach. In contrast, deploying larger models such as Phi 4 reasoning 14B may incur higher computational cost without providing additional performance gains.

#### F. Complexity Analysis & Deployment Considerations

This subsection presents the computational complexity of the proposed  $M$ -shot CoT-LLM mobile traffic prediction framework.

During the offline phase, for a raw dataset with  $H$  seconds of traffic measurements, the overall complexity of constructing the historical windows (i.e., forming  $[\Gamma, \mathbf{C}]$ ) with  $K$  contextual features is  $\mathcal{O}(H \cdot N \cdot K)$ , where  $N$  is defined in (11). Next, to generate the *rationales* for each training example, we invoke the LLM three times per sample, resulting in a total of  $3N$  LLM calls.

In contrast, during the online phase, after establishing the processed training set and using the policy  $\pi$ , the example-selection step requires  $\mathcal{O}(N \cdot M)$  operations for  $M$ -shot CoT-LLM. This is followed by a single LLM call with  $\approx 854$  input and  $\approx 152$  output tokens (output *rationale* + answer for 2-shot) per test sample to produce the prediction, which is suitable for close to real-time, online operation. In practice, the traffic prediction and LLM inference can be executed at the BSs or on cloud servers, where such platforms are typically equipped with graphics processing units and artificial intelligence acceleration hardware to efficiently support the computational demands of LLMs. Moreover, leveraging open-weight models, as demonstrated in the previous subsection,

<sup>2</sup>Note that at the time this research is conducted these are the state of the art models

enables network providers to deploy LLMs locally, thereby reducing both latency and the cost associated with external APIs. Under these infrastructure settings, an LLM with fewer than 15 billion parameters is expected to achieve an inference time of roughly 100 ms [38], while the corresponding communication latency can be around 50 ms [39], depending on the hardware configuration and network conditions. These delays remain within acceptable limits for per-second traffic prediction.

In summary, the proposed  $M$ -shot CoT-LLM approach is feasible for real-world deployment in 5G and 6G networks, offering acceptable latency and manageable hardware requirements.

## V. CONCLUSION

In this paper, we developed CoT-enabled LLM based mobile traffic prediction using real-world 5G measurements across different applications and mobility conditions. To address the limitations of standard ICL prompting for numerical time-series prediction, we proposed a two-phase framework with an offline phase and an online phase. In the offline phase, we create structured CoT demonstrations by generating rationales through a PCoT pipeline. In the online phase, we use a lightweight example-selection policy to retrieve the most relevant demonstrations by comparing both the historical throughput trajectory and its short-term changes. This design allows effective few-shot inference while keeping the prompt length limited.

Our results show that the proposed CoT-LLM approach can improve prediction accuracy and produce more stable outputs compared to ICL-LLM prompting and common baseline methods. In particular, the 2-shot CoT-LLM achieves improvements of up to 14.88%, 15.03%, and 22.41% in MAE, RMSE, and  $R^2$ -score, respectively. We further show that optimizing the number of in-context examples yields additional gains across MAE, RMSE, and  $R^2$ -score. In addition, tests with multiple open-weight LLMs indicate that locally deployable models can provide competitive performance, which reduces reliance on external API services and supports close to real-time prediction. For future work, more advanced reasoning prompting strategies can be explored.

## ACKNOWLEDGMENT

This work has been supported by MITACS, Ericsson Canada, and Canada Research Chairs program.

## REFERENCES

- [1] E. Lykakis, I. O. Vardiambasis, and E. Kokkinos, "Data traffic prediction for 5G and beyond: Emerging trends, challenges, and future directions: A scoping review," *Electronics*, vol. 14, no. 23, p. 4611, 2025.
- [2] W. Saad, M. Bennis, and M. Chen, "A vision of 6G wireless systems: Applications, trends, technologies, and open research problems," *IEEE Commun. Mag.*, vol. 58, no. 9, pp. 74–80, 2020.
- [3] F. Jiang, C. Pan, K. Wang, P. Michiardi, O. A. Dobre, and M. Debbah, "From large AI models to agentic AI: A tutorial on future intelligent communications," *IEEE J. Sel. Areas Commun.*, vol. 44, pp. 3507–3540, 2026.
- [4] D. A. Tedjopurnomo, Z. Bao, B. Zheng, F. M. Choudhury, and A. K. Qin, "A survey on modern deep neural network for traffic prediction: Trends, methods and challenges," *IEEE Trans. Knowl. Data Eng.*, vol. 34, no. 4, pp. 1544–1561, 2022.
- [5] X. Yin, G. Wu, J. Wei, Y. Shen, H. Qi, and B. Yin, "Deep learning on traffic prediction: Methods, analysis, and future directions," *IEEE Trans. Intell. Transp. Syst.*, vol. 23, no. 6, pp. 4927–4943, 2022.
- [6] P. E. Iturria-Rivera, M. Chenier, B. Herscovici, B. Kantarci, and M. Erol-Kantarci, "RI meets multi-link operation in ieee 802.11be: Multi-headed recurrent soft-actor critic-based traffic allocation," in *Proc. IEEE Int. Conf. Commun. (ICC) 2023*, 2023, pp. 4001–4006.
- [7] T. B. Brown, B. Mann, N. Ryder, M. Subbiah, J. Kaplan *et al.*, "Language models are few-shot learners," *Adv. Neural Inf. Process. Syst. (NeuroIPS)*, vol. 33, pp. 1877–1901, 2020.
- [8] J. Wei, X. Wang, D. Schuurmans, M. Bosma, b. ichter, F. Xia, E. Chi, Q. V. Le, and D. Zhou, "Chain-of-thought prompting elicits reasoning in large language models," in *Adv. Neural Inf. Process. Syst. (NeuroIPS)*, vol. 35, 2022, pp. 24 824–24 837.
- [9] B. L. Dalmazo, J. a. P. Vilela, and M. Curado, "Performance analysis of network traffic predictors in the cloud," *J. Netw. Syst. Manage.*, vol. 25, no. 2, p. 290–320, Apr. 2017.
- [10] Z. Tian and F. Li, "Network traffic prediction method based on autoregressive integrated moving average and adaptive volterra filter," *Int. J. Commun. Sys.*, vol. 34, no. 12, 2021. [Online]. Available: <https://doi.org/10.1002/dac.4891>
- [11] H. D. Trinh, L. Giupponi, and P. Dini, "Mobile traffic prediction from raw data using LSTM networks," in *Proc. IEEE Int. Symp. Personal, Indoor and Mobile Radio Commun. (PIMRC)*. Bologna, Italy: IEEE, 2018, pp. 1–6.
- [12] L. Bai, L. Yao, C. Li, X. Wang, and C. Wang, "Adaptive graph convolutional recurrent network for traffic forecasting," in *Proc. Annual Conf. Neural Inf. Process. Syst. (NeurIPS)*, 2020.
- [13] Y. Fang, S. Ergüt, and P. Patras, "SDGNet: A handover-aware spatiotemporal graph neural network for mobile traffic forecasting," *IEEE Commun. Lett.*, vol. 26, no. 3, pp. 582–586, 2022.
- [14] A. Vaswani, N. Shazeer, N. Parmar, J. Uszkoreit, L. Jones, A. N. Gomez, Ł. Kaiser, and I. Polosukhin, "Attention is all you need," in *Adv. Neural Inf. Process. Syst. (NeuroIPS)*, 2017, pp. 5998–6008.
- [15] G. Kougiumtzidis, V. K. Poulkov, P. I. Lazaridis, and Z. D. Zaharis, "Mobile network traffic prediction using temporal fusion transformer," *IEEE Trans. Artif. Intell.*, vol. 6, no. 10, pp. 2685–2699, 2025.
- [16] Y. Hu, Y. Zhou, J. Song, L. Xu, and X. Zhou, "Citywide mobile traffic forecasting using spatial-temporal downsampling transformer neural networks," *IEEE Trans. Netw. Serv. Manage.*, vol. 20, no. 1, pp. 152–165, 2023.
- [17] J. Gong, Y. Liu, T. Li, J. Ding, Z. Wang, and D. Jin, "STTF: A spatiotemporal transformer framework for multi-task mobile network prediction," *IEEE Trans. Mobile Comput.*, vol. 24, no. 5, pp. 4072–4085, 2025.
- [18] B. Gu, J. Zhan, S. Gong, W. Liu, Z. Su, and M. Guizani, "A spatial-temporal transformer network for city-level cellular traffic analysis and prediction," *IEEE Trans. Wireless Commun.*, vol. 22, no. 12, pp. 9412–9423, 2023.
- [19] H. Zhou, C. Hu, Y. Yuan, Y. Cui, Y. Jin, C. Chen, H. Wu, D. Yuan, L. Jiang, D. Wu, X. Liu, C. Zhang, X. Wang, and J. Liu, "Large language model (LLM) for telecommunications: A comprehensive survey on principles, key techniques, and opportunities," *IEEE Commun. Surveys Tuts.*, vol. 27, no. 3, pp. 1955–2005, 2024.
- [20] H. Zhang, A. B. Sediq, A. Afana, and M. Erol-Kantarci, "Large language models in wireless application design: In-context learning-enhanced automatic network intrusion detection," in *Proc. IEEE Global Commun. Conf. (GLOBECOM)*, 2024, pp. 2479–2484.
- [21] H. Zhang, A. Bin Sediq, A. Afana, and M. Erol-Kantarci, "Mobile traffic prediction using LLMs with efficient in-context demonstration selection," *IEEE Transactions on Communications*, vol. 73, no. 11, pp. 11 170–11 185, 2025.
- [22] C. Hu, H. Zhou, D. Wu, X. Chen, J. Yan, and X. Liu, "Self-refined generative foundation models for wireless traffic prediction," *IEEE Trans. Veh. Technol.*, 2025.
- [23] M. A. Habib, P. E. Iturria Rivera, Y. Ozcan, M. H. M. Elsayed, M. Bavand, R. Gaigalas, and M. Erol-Kantarci, "LLM-based intent processing and network optimization using attention-based hierarchical reinforcement learning," in *Proc. 2025 IEEE Wireless Commun. Netw. Conf. (WCNC)*, 2025, pp. 1–6.
- [24] D. Cao, F. Jia, S. O. Arik, T. Pfister, Y. Zheng, W. Ye, and Y. Liu, "Tempo: Prompt-based generative pre-trained transformer for time series forecasting," in *Proc. Int. Conf. Learn. Represent. (ICLR)*, 2024.
- [25] C. Chang, W.-Y. Wang, W.-C. Peng, and T.-F. Chen, "LLM4TS: Aligning pre-trained LLMs as data-efficient time-series forecasters," *ACM Trans. Intell. Syst. Technol.*, vol. 16, no. 3, pp. 1–20, 2025.

- [26] L. Huang, Y. Wu, and D. Simeonidou, "Reasoning AI performance degradation in 6G networks with large language models," in *Proc. 2025 IEEE Wireless Commun. Netw. Conf. (WCNC)*, 2025, pp. 1–6.
- [27] X. Wang, J. Zhu, R. Zhang, L. Feng, D. Niyato, J. Wang, H. Du, S. Mao, and Z. Han, "Chain-of-thought for large language model-empowered wireless communications," *arXiv preprint arXiv:2505.22320*, 2025.
- [28] T. Kojima, S. Gu, M. Reid, Y. Matsuo, and Y. Iwasawa, "Large language models are zero-shot reasoners," in *Adv. Neural Inf. Process. Syst. (NeuroIPS)*, vol. 35, 2022, pp. 22 199–22 213.
- [29] Q. Dong, L. Li, D. Dai, C. Zheng, J. Ma, R. Li, H. Xia, J. Xu, Z. Wu, B. Chang *et al.*, "A survey on in-context learning," in *Proc. 2024 Conf. Empir. Methods Nat. Lang. Process.*, 2024, pp. 1107–1128.
- [30] L. Wang, W. Xu, Y. Lan, Z. Hu, Y. Lan, R. K.-W. Lee, and E.-P. Lim, "Plan-and-solve prompting: Improving zero-shot chain-of-thought reasoning by large language models," in *Proc. 61st Annu. Meeting Assoc. Comput. Linguistics*, Toronto, Canada, 2023, pp. 2609–2634.
- [31] D. Raca, D. Leahy, C. J. Sreenan, and J. J. Quinlan, "Beyond throughput, the next generation: A 5G dataset with channel and context metrics," in *Proc. 11th ACM Multimedia Syst. Conf. (MMSys '20)*. ACM, 2020, pp. 303–308.
- [32] L. Mei, J. Gou, Y. Cai, H. Cao, and Y. Liu, "Realtime mobile bandwidth and handoff predictions in 4G/5G networks," *Comput. Netw.*, vol. 204, p. 108736, Feb. 2022.
- [33] OpenAI, "Openai o3 and o4-mini system card," 2025.
- [34] C. Bandt and B. Pompe, "Permutation entropy: A natural complexity measure for time series," *Physical Review Letters*, vol. 88, no. 17, p. 174102, 2002.
- [35] Mistral AI, "Minstral 3 3b," Mistral Docs (Open v25.12), Dec. 2025, accessed 2025-12-28.
- [36] A. Yang *et al.*, "Qwen3 technical report," *arXiv preprint arXiv:2505.09388*, 2025.
- [37] M. Abdin *et al.*, "Phi-4-reasoning technical report," *arXiv preprint arXiv:2504.21318*, 2025.
- [38] K. Chitty-Venkata *et al.*, "LLM-inference-bench: Inference benchmarking of large language models on AI accelerators," in *Proc. SC24-W: Workshops Int. Conf. High Perform. Comput., Netw., Storage Anal.*, Atlanta, GA, USA, 2024, pp. 1362–1379.
- [39] W. Fan, F. Xiao, Y. Pan, X. Chen, L. Han, and S. Yu, "Latency-aware joint task offloading and energy control for cooperative mobile edge computing," *IEEE Trans. Serv. Comput.*, vol. 18, no. 3, pp. 1515–1528, 2025.